

## Transactions Papers

# Transmission of Analog Signals Using Multicarrier Modulation: A Combined Source-Channel Coding Approach

Keang-Po Ho, *Member, IEEE*, and Joseph M. Kahn, *Member, IEEE*

**Abstract**—We have proposed and analyzed a combined source-channel coding scheme using multicarrier modulation. By changing the power and modulation of subchannels carrying different bits of the quantized signal, the channel-induced distortion can be minimized. We derive an algorithm for the allocation of power among subchannels. Analog sources quantized by scalar and vector quantizers are considered. For a Gaussian source scalar-quantized to 8 b, multicarrier transmission yields a 13 dB improvement of signal-to-distortion ratio over a single-carrier system. Quantizers having a smaller number of bits yield smaller improvements. We consider both full-search and binary tree-search vector quantizers using a natural binary coding scheme. For a vector quantizer using 2 b/sample, multicarrier transmission yields an improvement in signal-to-distortion ratio that lies between 0.3 and 0.8 dB, depending on the quantizer design.

### I. INTRODUCTION

ONE of the most important results of Shannon's work was that source coding and channel coding can be performed separately without sacrificing fidelity [1], [2]. Traditionally, the source and channel codes are designed separately and then cascaded together. However, Shannon's argument is true only if both transmitter and receiver are permitted to have an infinite degree of complexity. In practice, because of channel-induced additive noise, the probability of bit error [bit-error rate (BER)] is not infinitesimally small. In typical communication systems, in order to transmit an analog source, the source is quantized into binary bits and all bits are transmitted via the same channel, and are thus afforded the same protection against error. However, some bits in the quantized signal (e.g., the most significant bit of a scalar-quantized signal) are far more important than others. In such situation, we can combine the

source and channel codes into a single code in which the objective is to minimize the overall distortion between the original source at the transmitter and its reconstruction at the receiver.

Most studies of combined source-channel coding for continuous-amplitude sources lead to the study of quantizers for noisy channels. Design algorithms for either optimum scalar or vector quantizers operating over noisy channels were developed in [3]–[8]. Those algorithms optimize the quantizer under the assumption of a fixed noisy channel, usually a binary symmetric channel having a fixed transition probability. However, the modulation scheme of the channel can be changed along with the quantizer to provide unequal error protection for different bits. In this paper, we propose a simple yet powerful scheme for combined source-channel coding using multicarrier modulation. Multicarrier modulation [9]–[11] provides the flexibility to change the power, modulation, and channel encoding of each individual subchannel, so that different degrees of error protection may be provided for different bits, according to their importance. The distortion between the received signal and the original signal can be thereby minimized. Due to the complexity of joint optimization of the quantizer and channel modulation, we first choose an optimized quantizer, and then we optimize the channel modulation to minimize overall distortion. In this work, we assume that the channel is a static channel.

Multicarrier modulation is currently being considered as a standard channel-coding scheme for asymmetric digital subscriber lines (ADSL) [12]–[14], digital audio and high-definition television (HDTV) broadcasting [15]–[17] and wireless personal communication networks [10], [18]. Multicarrier modulation yields two important advantages [13] over single-carrier schemes. Firstly, a multicarrier signal can be processed in a receiver without the enhancement of noise or interference. Secondly, the long symbol time used in multicarrier modulation yields a much greater immunity to impulse noise and fast fades. In this paper, we demonstrate a third advantage of multicarrier modulation: it enables the use of combined source-channel coding in a natural way, without an increase of complexity in either the transmitter or the receiver. It should

Paper approved by E. Ayanoglu, the Editor for Communication Theory and Coding Application of the IEEE Communications Society. Manuscript received June 27, 1995; revised December 1, 1995 and March 12, 1996. This paper was supported by the Hughes Aircraft Company and by National Science Foundation Presidential Young Investigator Award ECS-9157089. This work was conducted at the University of California at Berkeley.

K.-P. Ho is with Bellcore, Red Bank, NJ 07701 USA (email: kpho@bellcore.com).

J. M. Kahn is with the Department of Electrical Engineering and Computer Sciences, University of California, Berkeley, CA 94720 USA (email: jmk@eecs.Berkeley.EDU).

Publisher Item Identifier S 0090-6778(96)08599-6.

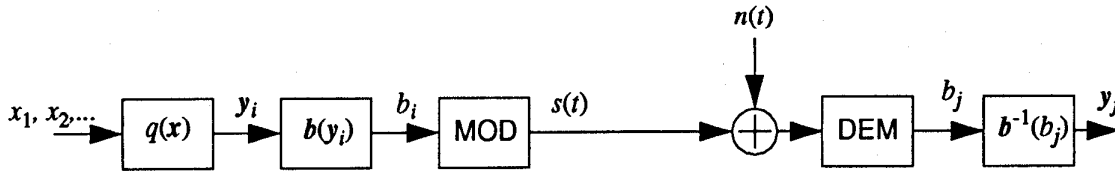


Fig. 1. Schematic diagram of a data-transmission system for an analog discrete-time source. At the transmitter, the source is quantized by either a scalar or vector quantizer to codewords, which are mapped to bits that drive a modulator. The receiver demodulates the signal to bits and returns the codewords. The input codeword  $y_i$  and output codeword  $y_j$  may be different due to bit errors. [modulator (MOD), demodulator (DEM)]

be noted, however, that multicarrier modulation is complicated to implement and is more sensitive to frequency offset, phase noise, and system nonlinearities [19].

The remainder of this paper is organized as follows. Section II provides a mathematical model for the combined source-channel coding scheme using multicarrier modulation. The general methods of quantizer design and analysis of channel-induced-distortion are reviewed. Algorithms for subchannel power allocation are given and the asymptotic gain in channel-induced-distortion is derived. Section III presents the application of the models of Section II to the optimal Lloyd–Max scalar quantizer. Section IV discusses the natural binary codeword assignment in a vector quantizer and presents the improvement achieved by multicarrier systems over single-carrier systems. Section V presents some examples of how the subchannel constellations can be modified to improve performance. Discussions and conclusions are given in Section VI and Section VII, respectively.

## II. COMBINED SOURCE-CHANNEL CODING SCHEME

Here we assume that the analog source to be transmitted is a real-valued, discrete-time, continuous-amplitude, stationary random process  $\{X_i; i = 0, 1, \dots\}$ . In this section, we first discuss methods of quantizer design and the effect of channel bit errors on the overall distortion, then discuss the algorithm for subchannel power allocation, and finally, we present an analysis of the asymptotic performance gain.

### A. Quantizer Design

The source can be encoded by means of a scalar quantizer [20]–[21] or a vector quantizer [22]–[23]. We assume that  $\mathbf{x} = (\mathbf{x}_{ik}, \mathbf{x}_{ik+1}, \dots, \mathbf{x}_{ik+k-1})$  represents the  $k$ -dimensional source vector. In vector quantization, the vector  $x$  is mapped to another real-valued, discrete-amplitude,  $k$ -dimensional vector  $y$ . We can write the quantization operator as  $q$ , so that

$$\mathbf{y} = \mathbf{q}(\mathbf{x}). \quad (1)$$

The output  $\mathbf{y}$  is called the *reconstruction vector*, *output vector*, *codeword*, or *codevector* corresponding to the input  $\mathbf{x}$ . The output  $\mathbf{y}$  is drawn from a finite reproduction alphabet  $Y = \{\mathbf{y}_1, \mathbf{y}_2, \dots, \mathbf{y}_Q\}$ , where  $\mathbf{y}_i = (y_{i1}, y_{i2}, \dots, y_{ik})$ . The set  $Y$  is referred to as the *reproduction codebook*, and  $Q$  is the number of levels or the size of the codebook. It is obvious that a scalar quantizer is a special case of a vector quantizer having unit dimension ( $k = 1$ ), so hereafter, in this section, we make no distinction between scalar and vector quantizers. The quantizer  $q$  is defined by the codebook, together with

the partition of the input space into sets  $S_i, i = 1, 2, \dots, Q$ . Specifically, the mapping  $q(\cdot)$  is described by

$$q(\mathbf{x}) = \mathbf{y}_i, \quad \text{if } \mathbf{x} \in S_i, \quad i = 1, 2, \dots, Q. \quad (2)$$

Let us assume that the distortion caused by representing a source  $\mathbf{x}$  by a reconstruction vector  $y$ , is described by a nonnegative distortion measure  $d(x, y)$ . The performance of a quantizer is generally measured by the average distortion per sample  $D_S(q)$

$$D_S(q) = \frac{1}{k} \sum_{i=1}^Q \int_{S_i} p(\mathbf{x}) d(\mathbf{x}, \mathbf{y}_i) d\mathbf{x} \quad (3)$$

where  $p(\mathbf{x})$  is the  $k$ -dimension probability density function of the source vector. For a given source and a given number of levels  $Q$ , a quantizer  $q^*$  is said to be optimum if

$$D_S(q^*) \leq D_S(q), \quad \text{for all } q. \quad (4)$$

Various algorithms for the design of “good” scalar and vector quantizers have been developed [20]–[23]. In this paper, unless stated otherwise, we assume that once a scalar or vector quantizer  $q$  is designed, it is then fixed.

In a digital communication system, as shown in Fig. 1, the codewords  $y_1, y_2, \dots, y_Q$  of the quantizer are mapped to binary codewords for digital transmission. We consider fixed-length binary codewords<sup>1</sup> of length  $n = \log_2 Q$ . We define  $b(\mathbf{y}_i), i = 1, 2, \dots, Q$ , to be a nonnegative integer whose  $n$ -bit binary representation is the binary codeword assigned to  $\mathbf{y}_i$ . In typical cases, the binary codewords representing the output of the quantizer are transmitted over a noisy channel. We assume that the channel is memoryless and has finite input and output alphabets given by  $\{0, 1, \dots, Q - 1\}$ . We let the transition probabilities  $P(j | i), i, j = 0, 1, \dots, Q - 1$ , denote the probability that the binary number  $j$  is received, given that the binary number  $i$  is transmitted. Therefore, the average distortion per source sample, caused by channel bit errors is given by

$$D_C(b) = \frac{1}{k} \sum_{i=1}^Q \sum_{j=1}^Q P(\mathbf{y} = \mathbf{y}_i) P(b(\mathbf{y}_j) | b(\mathbf{y}_i)) d(\mathbf{y}_i, \mathbf{y}_j) \quad (5)$$

where  $P(\mathbf{y} = \mathbf{y}_i)$  is the *a priori* probability of the codeword  $\mathbf{y}_i$ .

<sup>1</sup>Variable-length binary coding, e.g., Huffman coding, is too difficult to analyze because of the dependence of distortion on previous bit errors and the catastrophic effect of packet synchronization errors.

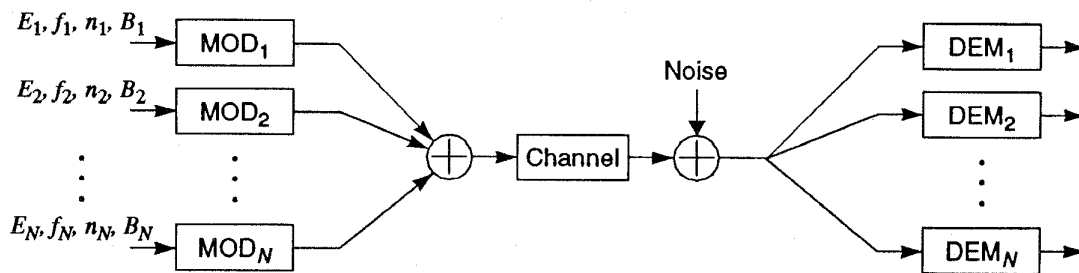


Fig. 2. Schematic diagram of a multicarrier system.  $E_m$  is the power transmitted in the  $m$ th subchannel,  $f_m$  is the center frequency of the  $m$ th subchannel,  $n_m$  is the number of bits per symbol of the  $m$ th subchannel, and  $B_m$  is the bandwidth of the  $m$ th subchannel.

The overall distortion caused by the quantizer and the channel is given by

$$D(q; b) = \frac{1}{k} \sum_{i=1}^Q \sum_{j=1}^Q P(b(y_j) | b(y_i)) \int_{S_i} p(x) d(x, y_j) dx \quad (6)$$

which, in general, is not equal to the sum of the source-encoder distortion  $D_S(q)$  and the channel-induced distortion  $D_C(q)$ . However, if the distortion criterion is the widely used squared-error distortion and if  $y_i$  is chosen to represent the centroid of the region  $S_i$ , the overall distortion is equal to the sum of the source-encoder distortion  $D_S(q)$  and the channel distortion  $D_C(q)$  [24]

$$D(q; b) = D_S(q) + D_C(b). \quad (7)$$

Therefore, to simplify our discussion, we will employ a squared-error distortion measure and choose each codeword to represent the centroid of its respective partition. The centroid condition is known to yield a quantizer that is optimal in the rate-distortion sense when the squared-error distortion measure is employed [20]–[23].

In view of this argument, once we have chosen a quantizer and a binary codeword assignment, we will then minimize the channel distortion  $D_C(q)$  by adjusting the transition probabilities  $P(j | i)$  through the choice of modulation scheme. This approach differs from the design of quantizers for noisy channels [3]–[8], in which the transition probabilities are fixed and given.

### B. Channel-Induced Distortion Using Multicarrier Modulation

When the communication channel becomes very noisy, it is a common practice to resort to some kind of error-correction coding scheme to reduce the effective channel bit-error probability. It is desirable to use error-correction coding so as to provide the highest level of protection to the most significant bit (MSB), since errors in the MSB induce the largest distortion. Likewise, lower levels of protection (or no protection at all) may be provided to less significant bits. However, error-correction coding requires the transmission of some redundant bits, and, in many implementations, increases the bandwidth required for transmission. Here, we seek to provide unequal error protection using a multicarrier modulation scheme.

Multicarrier modulation provides the flexibility to change the power, modulation, and channel encoding of each subchan-

nel on an individual basis, so that different error protection can be provided for different bits. The distortion between the original analog signal and the received signal can thereby be minimized. Assume that unequal error protection is provided so that the BER for the left-most bit is  $p_{b_1}$ , followed by  $p_{b_2}$  for the adjacent bit, and finally  $p_{b_n}$  for the right-most bit. Then, the transition probabilities are [25]

$$P(j | i) = \prod_{m=1}^n (1 - p_{b_m})^{1-l_m(i,j)} p_{b_m}^{l_m(i,j)} \quad i, j = 0, 1, \dots, Q-1 \quad (8)$$

where  $l_m(i, j) = 1$  if the binary codewords represented by  $i$  and  $j$  differ in the  $m$ th position, and otherwise  $l_m(i, j) = 0$ . It is obvious from this definition that the Hamming distance between codewords  $i$  and  $j$  is the sum of  $l_m(i, j)$ , or  $d_H(i, j) = \sum_{m=1}^n l_m(i, j)$ . If  $p_{b_1} \leq p_{b_2} \leq \dots \leq p_{b_n}$ , then the BER increases as one moves from left to right within a codeword. In this case, in the mapping of codewords  $y_i$  to binary codewords  $b(y_i)$ ,  $i = 1, 2, \dots, Q$ , left-side bits should be used to distinguish between codewords separated by a large Euclidean distance, whereas this should be avoided, as much as possible, for right-side bits.

The schematic diagram of a multicarrier modulation system is shown in Fig. 2. Each subchannel can utilize different power, modulation, channel encoding, and bandwidth. We will use  $N = n$  subchannels to transmit the  $n$ -bit signal,<sup>2</sup> assigning different bits to different subchannels in consecutive order. The BER  $p_{b_m}$  is a function of  $E_m$ , the power in the  $m$ th subchannel, i.e.,  $p_{b_m} = P_m(E_m)$ . The sum of these powers is equal to the total power  $E_T$ . The BER functions  $P_m(\cdot)$  may be different for each subchannel, depending on the choice of modulation and channel encoding. Therefore, the objective function to be minimized is the channel-induced-distortion of (5) in which  $P(j | i)$  is given by (8) and  $p_{b_m} = P_m(E_m)$ . However, this objective function is too difficult to optimize directly, and we seek to simplify it further.

<sup>2</sup> $N$  need not equal  $n$ , nor does it even need to be an integral multiple of  $n$ . For example, we may utilize three subchannels for the left-most bit, one subchannel for the second bit, etc. However, usually, identical error rates should be achieved by all subchannels conveying a given bit (e.g., the three subchannels conveying the left-most bit), implying that they should employ identical modulation, error-correction coding and signal-to-noise ratio (SNR). In our mathematical description, without loss of generality, we can describe all subchannels conveying a given bit as a single subchannel and thus, the number of subchannels and number of bits are taken to be equal ( $N = n$ ). Note, that this argument is true only if the spectral density of the channel noise is white.

Usually the BER's  $p_{b_1}, p_{b_2}, \dots, p_{b_n}$  are small, so that the probability of multiple bit errors within the same binary codewords is very small. This permits us to ignore any terms having factors of  $p_{b_{m_1}} p_{b_{m_2}}, m_1, m_2 = 1, 2, \dots, n$ , which simplifies the transition probabilities given by (8) to

$$P(j | i) \approx \begin{cases} 1 & i = j \\ p_{b_m} & l_m(i, j) = 1, d_H(i, j) = 1 \\ 0 & d_H(i, j) > 1. \end{cases} \quad (9)$$

In this simplification,  $P(j | i)$  is nonzero if  $i$  and  $j$  are equal, or are separated by a unit Hamming distance, i.e.,  $d_H(i, j) = 1$ . Considering the terms with  $P(j | i) \neq 0$  and  $i \neq j$ , for any  $n$ -bit binary number  $i$ , there are  $n$  different binary numbers separated from  $i$  by a unit Hamming distance. If  $i_m$  is the  $m$ th bit in the binary representation of  $i$ , i.e.,  $i = \sum_{m=1}^n i_m 2^{n-m}$ , those  $n$  binary numbers are  $i_{e_m} = i + (1 - 2i_m)2^{n-m}$ ,  $m = 1, 2, \dots, n$ . Therefore, after some algebra, the channel-induced distortion (5) is

$$D_C(b; E_m) = \frac{1}{k} \sum_{i=0}^{Q-1} \sum_{m=1}^n P(\mathbf{y} = b^{-1}(i)) P_m(E_m) \times \|b^{-1}(i) - b^{-1}(i_{e_m})\|^2. \quad (10)$$

Exchanging the order of summation, we would like to minimize the channel distortion

$$D_C(b; E_m) = \frac{1}{k} \sum_{m=1}^n P_m(E_m) W_m \quad (11)$$

subject to the constraint

$$\sum_{m=1}^n E_m = E_T \quad (12)$$

where  $W_m$  is the weighting factor of the  $m$ th bit

$$W_m = \sum_{i=0}^{Q-1} P(\mathbf{y} = b^{-1}(i)) \|b^{-1}(i) - b^{-1}(i_{e_m})\|^2. \quad (13)$$

Note that, for one-dimensional scalar quantizer, these weighting factors are similar to the  $A$ -factors in [26]–[28]. However, we are concerned here with optimal vector (or scalar) quantizers, instead of standard companding techniques.

For a given quantizer, the weighting factors  $W_m$ ,  $m = 1, 2, \dots, n$ , are independent of the channel and can be evaluated once the quantizer (include the bit mapping) is specified. The design of channel modulation depends on the quantizer design, but the quantizer design is independent from the channel, and once the quantizer is designed, the information required to design the channel modulation is summarized in the weighting factors  $W_m$ ,  $m = 1, 2, \dots, n$ . Assuming that the bits decrease in significance as one moves from left to right within a binary codeword, we expect that  $W_1 \geq W_2 \geq \dots \geq W_n$ . The mapping to binary codewords  $b(\mathbf{y}_i)$  determines the location significance of bits within the binary codeword. Below, we will discuss the mapping to binary codewords that is appropriate for specific quantizer designs

### C. Power Allocation for Multicarrier Modulation

Different subchannels may be afforded unequal error protection by changing the modulation constellation without changing the power (for example, from 16-QAM to 32-QAM). However, typically, for the same power, a change of modulation scheme induces an excessively large change in BER. Therefore, we will change the power of the subchannels to provide unequal error protection. Similar to the approach of [32] introducing a Lagrange multiplier  $\lambda$ , we would like to find the subchannel power allocation to minimize

$$H(E_m, \lambda) = \sum_{m=1}^n W_m P_m(E_m) - \lambda \sum_{m=1}^n E_m. \quad (14)$$

The solution is

$$W_m \frac{dP_m(E_m)}{dE_m} = \lambda \quad m = 1, 2, \dots, n \quad (15)$$

$$\sum_{m=1}^n E_m = E_T.$$

A power allocation similar to (15) was considered in [32] for a one-dimensional uniform quantizer. However, our problem is more general, since we consider vector quantizers and multicarrier modulation schemes.

Expressing  $dP_m(E_m)/dE_m = G_m(E_m)$ , we have  $E_m = G_m^{-1}(\lambda/W_m)$ ,  $m = 1, \dots, n$ . We assume that both  $G_m(\cdot)$  and  $G_m^{-1}(\cdot)$  can be evaluated using either numerical or analytical techniques. If we are given a specific value of the total power  $E_T$ , we may solve a one-dimensional nonlinear equation

$$\sum_{m=1}^n G_m^{-1}(\lambda/W_m) = E_T \quad (16)$$

by numerical methods to find  $\lambda$ . For a Gaussian channel,  $G_m^{-1}(\cdot)$  is usually a monotonic function, so that the Lagrange multiplier  $\lambda$  in (16) can be obtained by the use of a bisection method. Although the power allocation solution (15) makes use of the simplification provided by (9), to improve the accuracy, the calculation of channel distortion  $D_C(b; E_m)$  can instead be performed using (5) with transition probabilities given by (8). However, as shown later, for the range of signal powers that we consider, there is no significant difference between values of the channel distortion  $D_C(b; E_m)$  computed using the transition probabilities (8) and those computed using (9), especially when the number of quantization levels  $Q$  is large.

### D. Asymptotic Gains for Gaussian Channel

Here we derive the asymptotic gain in signal-to-channel-induced-distortion ratio ( $S/D_C$ ) for a Gaussian channel at high SNR. For simplicity, we assume that all subchannels use identical modulation, occupy identical bandwidth, and are transmitted over an additive white Gaussian noise (AWGN) channel. Using binary phase-shift-keying (BPSK), the BER is [29]

$$p_b = \frac{1}{2} \operatorname{erfc}(\sqrt{\rho}) \quad (17)$$

where  $\rho$  is the SNR of the channel. Assuming coherent detection on an AWGN channel and high SNR, for square  $M$ -QAM, the symbol-error rate  $p_S$  is tightly upper-bounded as  $p_S < 2(1 - 1/\sqrt{M})\text{erfc}(\sqrt{\rho/\beta})$  [29, p. 283], while for  $M$ -PSK, a good approximation is  $p_S < \text{erfc}(\sqrt{\rho/\beta})$  [29, p. 265].  $\beta$  is a constant that depends upon the modulation scheme. When a Gray code is used in the mapping from bits to symbols, adjacent constellation points differ in only a single encoded bit. Since the most probable errors due to noise result in the erroneous selection of a point adjacent to the correct point, most symbol errors cause only a single bit error, and we may make the approximation  $p_b \approx p_S/\log_2 M$ , where  $p_S$  is the symbol-error rate. Hence, for either QAM or PSK, the BER can be approximately expressed as

$$p_b \approx (\alpha/2)\text{erfc}(\sqrt{\rho/\beta}) \quad (18)$$

where  $\alpha$  and  $\beta$  are constants that depend on the modulation scheme.

The SNR of the  $m$ th subchannel of a multicarrier system in an AWGN channel is  $\rho_m = E_m/(N_0 B_m)$ , where  $N_0$  is the noise power spectral density, assumed to be identical for each subchannel. The average SNR of the multicarrier system is  $\rho_T = E_T/(N_0 B_T)$ , where  $B_T$  is the total bandwidth of the multicarrier signal. Besides these simple modulation schemes, one may employ more complicated subchannel modulation schemes, including the addition of error-correction coding, or the use of trellis-coded modulation or continuous-phase modulation [29]. Without loss of generality, we assume that all subchannels employ identical BPSK modulation. The average SNR is simply the arithmetic mean of the SNR's of the individual subchannels, i.e.,  $\rho_T = (\sum_{m=1}^n \rho_m)/n$ .

Under the assumption of high SNR,  $p_b \approx \frac{1}{2}e^{-\rho}/\sqrt{\pi\rho}$ . Therefore,  $dp_b/d\rho \approx \frac{1}{2}e^{-\rho}/\sqrt{\pi\rho} = p_b$ . The solution provided by (15) becomes  $W_m p_{b_m} \approx \lambda N_0 B$ . This expression has the obvious interpretation that all bits contribute equally to the total channel-induced distortion. With some algebra, it can be shown that at high SNR

$$E_{m1} - E_{m2} \propto \log(W_{m1}/W_{m2}). \quad (19)$$

Because the difference between the powers in two subchannels is a constant, at large SNR, the power of each subchannel should be approximately the same, so that  $E_{m1}/E_{m2} \approx 1$  or  $\rho_{m1}/\rho_{m2} \approx 1$ .

If only a single carrier is employed, the BER of the system is  $p_{b_T} \approx \frac{1}{2}e^{-\rho_T}/\sqrt{\pi\rho_T}$ . Thus

$$p_{b_T} = \frac{\exp[-(\sum_{m=1}^n \rho_m)/n]}{2\sqrt{\pi\rho_T}} \approx \left(\prod_{m=0}^n p_{b_m}\right)^{1/n}. \quad (20)$$

In (20), we use the approximation  $\rho_m/\rho_T \approx 1, m = 1, \dots, n$ , which is valid for high SNR. Expressing the reduction of channel-induced distortion  $D_C(b; E_m)$  in terms of the gain in signal-to-channel-induced-distortion ratio ( $S/D_C$ ), the gain achieved by multicarrier transmission over single-carrier transmission is

$$G_{E_T \rightarrow \infty} = \frac{p_{b_T} \sum_{m=1}^n W_m}{\sum_{m=1}^n W_m p_{b_m}}. \quad (21)$$

After some algebra, we can show that the gain is the ratio of the arithmetic and geometric means of  $W_m, m = 1, \dots, n$

$$G_{E_T \rightarrow \infty} = \frac{\frac{1}{n} \sum_{m=1}^n W_m}{(\prod_{m=1}^n W_m)^{1/n}}. \quad (22)$$

Note that the asymptotic gain in  $S/D_C$  given by (22) is valid only if all subchannels have identical modulations, bandwidths and Gaussian noises. It is invalid if different subchannels employ different modulations or have unequal bandwidths, noise powers, or gains (e.g., due to frequency-selective fading).

The combined source-channel coding scheme described here, like other combined source-channel coding schemes, is most effective at low-to-moderate SNR. While the asymptotic gain of  $S/D_C$  (22) is derived at high SNR, as shown later, it also provides a reasonable estimate of the gain of  $S/D_C$  at low-to-moderate SNR's. As we show below, at these low-to-moderate SNR's, where  $S/D$  is limited mainly by  $S/D_C$ , the gain (22) also provides a reasonable estimate of the gain of  $S/D$ .

### III. SCALAR LLOYD-MAX QUANTIZER

The design of an optimal scalar quantizer, or the Lloyd-Max quantizer, is addressed by Lloyd [20] and Max [21]. We can use either natural binary code (NBC) or folded binary code (FBC) for the binary encoding. At high SNR's and low BER's, FBC yields smaller distortion than NBC<sup>3</sup> for a Gaussian source. Table I shows the weighting factors  $W_m$ , MSE  $D_S(q)$ , and other parameters of optimal scalar quantizers from one to nine bits designed by Method I of Lloyd [20] for a zero mean, unit-variance Gaussian source, using NBC and FBC for binary encoding. Both NBC and FBC have the same weighting factors  $W_m$  for  $m$  larger than unity. At small BER's, NBC yields greater channel distortion than FBC because of the larger value of  $W_1$ . For a large number of levels, the quantizer can also be designed by the companding technique [30]–[31].

Fig. 3 presents the  $S/D$  obtained using an optimal quantizer of three through nine bits for transmission through an AWGN channel with uniform noise spectral density. All subchannels of the multicarrier system use identical BPSK modulation for simplicity. The power is allocated according to (15) and the subchannel SNR's change correspondingly. At small average SNR  $\rho_T$ , significant gain in  $S/D$  can be obtained. Fig. 4 shows the gain in  $S/D$  and  $S/D_C$  obtained by multicarrier modulation over single-carrier modulation for quantizers of three through nine bits. The gains in  $S/D_C$  obtained using multicarrier modulation increase with the average SNR  $\rho_T$  and approach asymptotic limits that are identical to the  $G_{E_T \rightarrow \infty}$  listed in Table I. In Fig. 4, we see that the maximum gains in  $S/D$  are also close to these asymptotic limits. It can be seen in Fig. 4 that the gain in  $S/D$  and  $S/D_C$  obtained using FBC is always smaller than that obtained using NBC. Fig. 3 shows that FBC always performs better than NBC at all values of average SNR. The improvement of FBC over NBC for single-carrier transmission is higher than that for multicarrier

<sup>3</sup>This is not true for other sources, e.g., NBC yields lower distortion than FBC for uniformly distributed source.

TABLE I  
WEIGHTING FACTORS  $W_m$  AND MSE  $D_S(q)$  FOR LLOYD-MAX QUANTIZERS OF ONE THROUGH NINE BITS, FOR A UNIT-VARIANCE GAUSSIAN SOURCE

Number of Levels, Q	2	4	8	16	32	64	128	256	512
NBC $W_1$ (dB)	4.061	5.859	7.015	7.748	8.205	8.484	8.651	8.750	8.812
FBC $W_1$ (dB)	4.601	5.478	5.868	5.979	6.010	6.018	6.020	6.020	6.020
$W_2$ (dB)		0.486	1.780	2.622	3.162	3.500	3.706	3.831	3.905
$W_3$ (dB)			-4.247	-3.451	-2.938	-2.609	-2.400	-2.270	-2.192
$W_4$ (dB)				-9.605	-9.153	-8.863	-8.674	-8.553	-8.478
$W_5$ (dB)					-15.293	-15.047	-14.890	-14.787	-14.720
$W_6$ (dB)						-21.148	-21.018	-20.935	-20.880
$W_7$ (dB)							-27.087	-27.019	-26.978
$W_8$ (dB)								-33.066	-33.032
$W_9$ (dB)									-39.063
NBC $G_{E_T \rightarrow \infty}$ (dB)	0	0.783	2.109	3.865	5.920	8.170	10.548	13.016	15.550
FBC $G_{E_T \rightarrow \infty}$ (dB)	0	0.681	1.688	3.122	4.927	6.999	9.254	11.635	14.106
MSE, $D_S(q)$ (dB)	-4.396	-9.300	-14.616	-20.222	-26.013	-31.910	-37.865	-43.853	-49.856

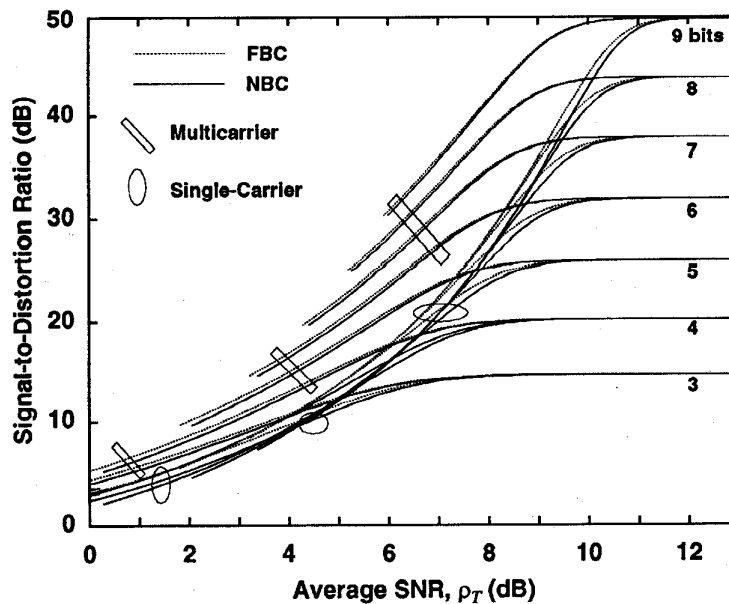


Fig. 3. Signal-to-overall distortion ratio  $S/D$ , as a function of the average SNR of an AWGN channel. The signal is a Gaussian source quantized by the optimal Lloyd-Max quantizer.

transmission. Therefore, in Fig. 4, the gain achieved using FBC is smaller than that obtained using NBC. The calculations of  $S/D$  and the gain in  $S/D$  in Figs. 3 and 4 are based on the simplification of (9), which is true at high average SNR, and thus at low BER. For the range of average SNR's we consider in Figs. 3 and 4, numerical result shows that there is no significant difference between results obtained using the transition probabilities (8) and (9).

The curves in Figs. 3 and 4 rely upon the assumption that all subchannels in the multicarrier modulation system use BPSK modulation. In practice, most multicarrier modulation systems use  $M$ -ary QAM modulation. For any QAM or PSK modulation scheme, the BER can be approximately expressed as (18). For other types of modulation, if  $\alpha$  is unity, all curves in Figs. 3 and 4 should be moved right by  $10 \cdot \log_{10}(\beta)$  dB. The curves of  $S/D$  of Fig. 3 and the gain of  $S/D$  in Fig. 4

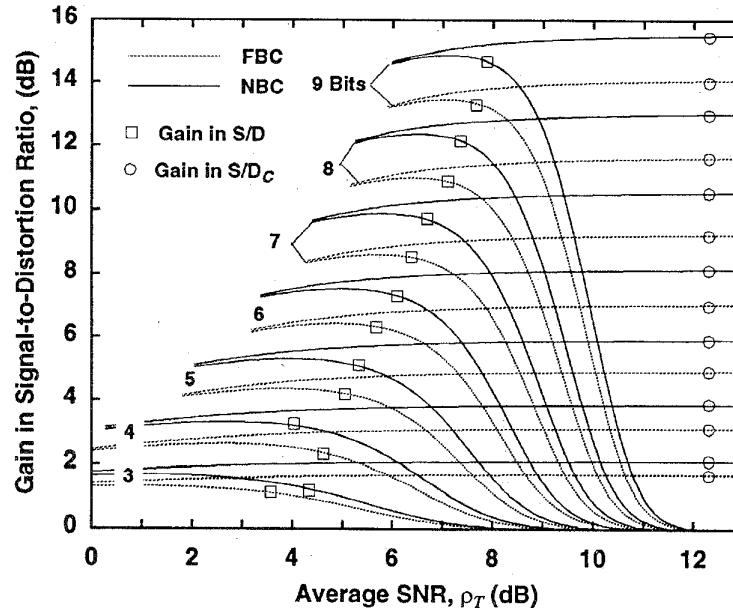


Fig. 4. Gain in the overall distortion ratio  $S/D$  and the signal-to-channel-induced distortion ratio  $S/D_C$ , as a function of the average SNR  $\rho_T$ . All parameters are the same as in Fig. 3.

need to be modified slightly in a straightforward fashion if  $\alpha$  is not unity. Note that the curves of the gain in  $S/D_C$  of Fig. 4 simply need to be moved right by  $10 \cdot \log_{10}(\beta)$  dB even  $\alpha$  is not unity.

#### IV. VECTOR QUANTIZER

There are various algorithms to design vector quantizers [22]–[23]. The popular LBG algorithm [33] is known to achieve the rate-distortion limit asymptotically. In order to achieve a large reduction in channel-induced distortion, asymptotically, from (22), the weighting factors of different bits must be different, because a difference implies the distinction between the significance of different bits that is necessary to achieve a gain in  $S/D$ . Therefore, the mapping to binary codewords must be done so that the important bits and unimportant bits are arranged in a hierarchical order.

For the LBG algorithm, one natural way to assign the binary codeword is the use of the “splitting” algorithm [33] for the initialization of the vector quantizer design algorithm. To design a  $n$ -bit quantizer with  $2^n$  codewords, we first compute the centroid of the entire training sequence, say  $y_0$ . Then we split  $y_0$  into  $y_0 + \delta y_0$  and  $y_0 - \delta y_0$  by a small perturbation  $\delta y_0$ . This will result into the partitioning of the set of training vectors into two sets for those training vectors that are closer to  $y_0 + \delta y_0$  and  $y_0 - \delta y_0$ , respectively. Using the LBG algorithm for these two initial codewords, we compute the two optimal codewords for this two-level vector quantizer, call them  $y_{10}$  and  $y_{11}$  and label them by “0” and “1,” respectively. In the same manner, we split each of  $y_{10}$  and  $y_{11}$  and compute the four new codewords, which we call  $y_{200}$ ,  $y_{201}$ ,  $y_{210}$ , and  $y_{211}$ , and which we label by “00,” “01,” “10,” and “11,” respectively. Clearly, if we continue in the same manner, and the number of codewords is doubled each time, we will end up

with the desired  $2^n$  codewords with natural binary codeword assignment.

However, a vector quantizer designed by the LBG algorithm [23] requires a large complexity in the encoding process, because of the need to use full-search algorithms. To reduce the complexity, a structured vector quantizer is usually employed. Here, we also consider the tree-structure vector quantizer using binary search tree [22]–[23] which is a natural by-product of the splitting algorithm. Compared with the LBG algorithm, the tree-structure vector quantizer requires about twice the memory, but yields a complexity reduction in the encoder from full-search to binary-search (from  $2^n$  comparisons to  $n$  comparisons). The training of the tree-structured vector quantizer is similar to the splitting algorithm described above. However, for example, at the second splitting, only the region closest to  $y_{10}$  is used to train  $y_{200}$  and  $y_{201}$ , and the region closest to  $y_{11}$  is used to train  $y_{210}$  and  $y_{211}$ , respectively. This is unlike the LBG algorithm, in which the whole space (or training sequence) is used to train  $y_{200}$ ,  $y_{201}$ ,  $y_{210}$ , and  $y_{211}$ . Furthermore, the intermediate codewords  $y_{10}$ ,  $y_{11}$ ,  $y_{200}$ , etc., need to be stored for the encoding and decoding process, hence the larger memory requirement. One natural way to encode the tree-structured vector-quantized codewords is to assign the left-most bit for the topmost tree structure and successive bits to the right of it to successively lower-level subtrees. The encoding of binary codewords is done so that a given bit is encoded to “0” or “1” if the search in the tree goes to a “left” or “right” sub-tree, respectively.

The parameters of the vector quantizers for an independent, identically distributed (i.i.d.) Gaussian, zero-mean, unit-variance source are given in Table II. The quantized rate is 2 b/sample, so that we encode vectors of dimensions  $k = 2, 3, 4$  using binary codewords of lengths  $n = 4, 6$ , and 8, respectively. Vector quantizers trained by both the LBG

TABLE II  
PARAMETERS OF VECTOR QUANTIZERS FOR A UNIT-VARIANCE I.I.D. GAUSSIAN SOURCE

Vector Quantizers	Full-Search LBG Algorithm			Tree-Structured Vector Quantizer		
	$k=2$	$k=3$	$k=4$	$k=2$	$k=3$	$k=4$
$W_1$ (dB)	5.093	8.949	8.485	6.406	8.395	9.310
$W_2$ (dB)	6.018	8.791	8.740	6.445	7.871	8.549
$W_3$ (dB)	4.837	7.822	8.751	3.135	6.929	7.656
$W_4$ (dB)	0.850	6.498	7.764	0.848	3.501	7.098
$W_5$ (dB)		3.538	6.878		2.130	4.306
$W_6$ (dB)		0.671	5.258		-0.092	3.498
$W_7$ (dB)			3.022			2.040
$W_8$ (dB)			0.130			-0.413
$G_{E_T \rightarrow \infty}$ (dB)	0.383	0.852	0.782	0.583	1.012	1.040
MSE, $D_S(q)$ (dB)	-9.600	-10.047	-10.518	-9.159	-9.329	-9.519

full-search algorithm and the binary tree-search algorithm are considered. The number of training vectors per quantizer level is 200 for  $k=2, 3$ , and 60 for  $k=4$ , as required to yield a good choice of codewords [34]. For a given dimension, an LBG vector quantizer yields smaller MSE than its tree-structured counterpart. For either type of quantizer, the MSE decreases as the dimension is increased. The two-dimensional (2-D) full-search vector quantizer performs 0.44 dB better than the 2-D tree-structured vector quantizer, and even 0.08 dB better than the four-dimensional (4-D) tree-structured vector quantizer. Considering tree-search vector quantizers, going from two to three dimensions yields a 0.45-dB decrease of MSE, while going to four dimensions decreases the MSE by an additional 0.47 dB.

As can be seen in Table II, the first bit in a codeword is not necessarily the MSB; however, bits at the left side of a codeword tend to be more significant than those at the right side, because the former tend to have larger weight factors  $W_m$ . Therefore, the natural binary codeword assignment produced by the splitting algorithm provides a natural assignment of the importance of each bit. We observe that the asymptotic gains of the multicarrier system on an AWGN channel are larger for a tree-structured vector quantizer than for a LBG quantizer of the same dimension. We thus conclude that the natural binary codeword assignment made by the binary search tree is superior to that made by the LBG algorithm.

Fig. 5 shows the signal-to-overall distortion ratio  $S/D$  as a function of the average SNR  $\rho_T$  for the vector quantizers of Table II, and for the four-level scalar quantizer ( $k=1$  and  $Q=4$ ) of Table I. When the average SNR  $\rho_T$  is smaller than about 8 dB,  $S/D$  decreases, due to the high BER. For low  $\rho_T$ , vector quantizers having low dimension actually perform better than vector quantizers having high dimension, especially for the tree-structured vector quantizer shown in Fig. 5(b). Comparing the three- and four-dimensional full-search and tree-structured vector quantizers in Fig. 5(a) and (b), respectively, at low SNR

$\rho_T$ , tree-structured vector quantizers perform better than their full-search counterparts. The superior performance at low SNR of tree-structured vector quantizers is due to their better natural binary codeword assignment, which results in better arrangement of weighting factors, as can be seen in Table II.

The asymptotic gains in channel-induced distortion are tabulated in Table II. Because the vector quantizers utilize the very low rate of 2 b/sample, the gains in overall distortion are of the order of 0.2 to 0.4 dB for the 2-D quantizers and 0.55 to 0.75 dB for the 3- and 4-D quantizers. The tree-structured vector quantizers yield larger gains than the corresponding full-search vector quantizers. Numerical results show that there is very little difference between values of  $S/D$  calculated using (8) and (9), especially for 3- and 4-D vector quantizers.

## V. SUBCHANNEL MODULATION SCHEME

All of the calculations above consider use of the same modulation scheme for all subchannels. The modulation schemes of different channels can be chosen differently to provide unequal error protection for different bits. If a high-level modulation scheme is used for the less-significant bits, the overall bandwidth required for multicarrier transmission can be reduced. Fig. 3 shows that, in general, quantizers employing more bits always provide superior performance. However, this is true only if the overall bandwidth used by the system is permitted to increase as the number of bits increases. In this section, we address the case where the bandwidth is held constant.

As an example, assume that the overall bandwidth  $B_T$  of the system is twice the sampling rate, or equivalently, the overall bandwidth is twice the number of samples per second. Using BPSK for all subchannels, a 2 b quantizer can be used. Using QPSK for all subchannels, a 4 b quantizer can be employed. However, for a 4 b quantizer, holding the overall bandwidth constant, we may instead use BPSK for the first bit, and 8-

QAM or 8-PSK for the remaining 3 b. As a more complicated example, we can use QPSK with a rate-2/3 convolutional code for the first bit, 8-QAM with a rate-4/7 convolutional code for the second bit, and uncoded 8-QAM for the third and fourth bits. The total bandwidth is twice the sampling rate, with the first, second, third, and fourth bits, occupying bandwidths of 3/4, 7/12, 1/3, and 1/3 times the sampling rate, respectively. The number of possible combinations is very large, and it may be difficult to identify an optimal scheme. Therefore, to limit the number of possible combinations, we consider only systems without error-correction coding.

Fig. 6 shows the  $S/D$  for a Gaussian source as a function of average SNR  $\rho_T$  for a system using a two-sided bandwidth equal to four times the sampling rate. The optimal scalar quantizers of 2–8 b from Table I are employed, the power used in each subchannel is determined by the solution of (15), and FBC binary encoding is employed for its better performance. Examining Fig. 6, we see that as  $\rho_T$  increases, the number of bits that the quantizer should employ increases. For comparison, Fig. 6 also shows the  $S/D$  achieved when all subchannels have equal SNR.

At low SNR, to maximize  $S/D$ , the analog signal must be quantized using a small number of bits. At the same time, a modulation having a small number of constellation points, such as BPSK or QPSK, should be employed for each subchannel in the multicarrier transmission system. At high SNR's, quantizers using a larger number of bits can be employed, and more complex constellations, such as 8-QAM or 16-QAM,<sup>4</sup> can be employed, so as to maintain the system bandwidth constant. For example, if the average SNR of the system is between 11 and 13.5 dB, an optimal scalar quantizer of 5 b can be employed. The first two of these 5 b can be transmitted on QPSK subchannels, and the remaining 3 b can be transmitted on 8-QAM subchannels. The required overall bandwidth remains four times the sampling rate. If the average SNR is larger than 13.5 dB, a 6 b quantizer can be employed for better performance, and the modulation scheme for each subchannel may be changed correspondingly.

While the subchannel modulation schemes shown in Fig. 6 represent reasonable choices, they may or may not be optimal for the range of SNR considered. For example, for an 8 b quantizer, further numerical results show that for an average SNR below 17.8 dB, the modulation scheme of 8-QAM + 6 × 16-QAM + 64-QAM (not shown in Fig. 6) provides better performance than the modulation scheme of 8 × 16-QAM; however, for average SNR above 17.8 dB, the opposite is true. Furthermore, we are unable to identify a general rule for determining the optimal subchannel modulation scheme. For example, for a 6 b quantizer, the QPSK + 3 × 8-QAM + 2 × 16-QAM scheme shown in Fig. 6 is better than the identical-constellation scheme 6 × 8-QAM over the whole range of average SNR between 12 and 20 dB. However, for

<sup>4</sup>We use the approximation (18) for  $M$ -ary QAM, and the approximate symbol-error rate is  $p_S = \text{erfc}(\sqrt{\rho/2})$  (for QPSK),  $p_S = \text{erfc}(\sqrt{\rho/6})$  (for 8-QAM consisting of a three-by-three square with the center point deleted), and  $p_S = 1.5 \text{erfc}(\sqrt{\rho/10})$  (for 16-QAM). Further numerical results show that over the range of SNR's considered in Fig. 6, approximating the BER by  $p_b \approx p_S / \log_2 M$  yields results indistinguishable from those obtained using the exact BER.

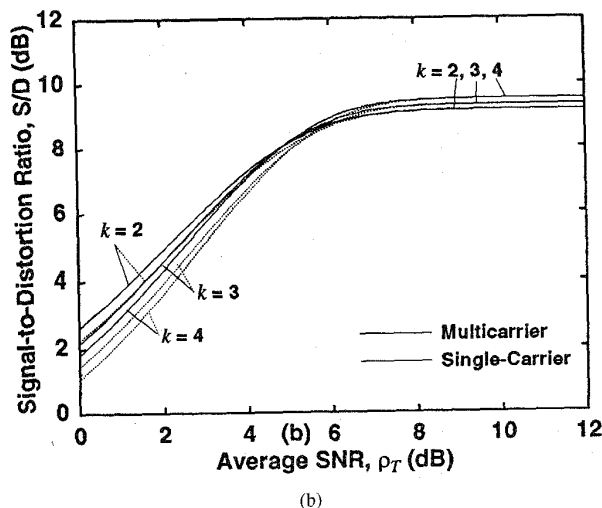
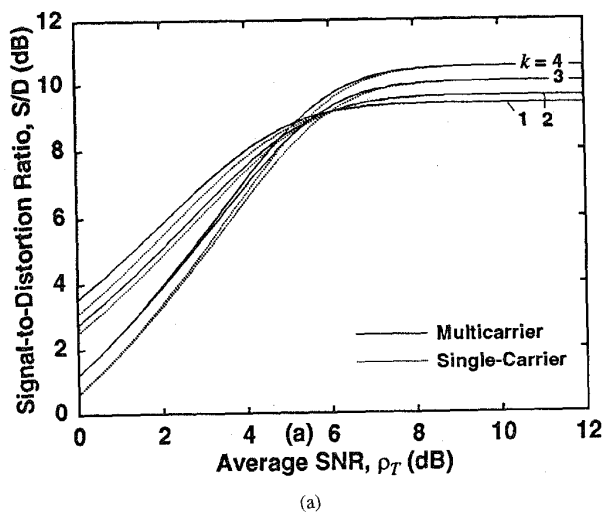


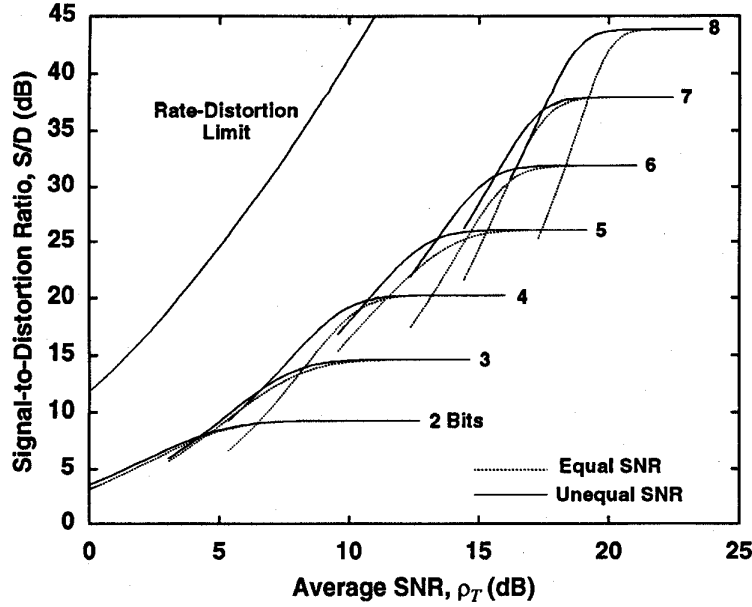
Fig. 5. The signal-to-distortion ratio  $S/D$ , as a function of the average SNR  $\rho_T$  of an AWGN channel. The signal is an i.i.d. Gaussian source, quantized by vector quantizers having rates of 2 b/sample and dimensions of  $k = 1, 2, 3, 4$ : (a) vector quantizer trained by full-search LBG algorithm (optimal scalar quantizer for  $k = 1$ ) and (b) tree-structured vector quantizer.

an 8 b quantizer, as discussed earlier, 8 × 16-QAM appears to be the best scheme for SNR's above 17.8 dB.

Fig. 6 also shows the rate-distortion  $S/D$  limit. The limit is calculated by  $S/D = 2^{2R}$ , and  $R = 2 \log_2(1 + \rho_T)$ . Our results are still far below the rate-distortion limit for two reasons: (a) QAM modulation cannot achieve the channel capacity of the AWGN channel; and (b) the Lloyd–Max scalar quantizer cannot achieve the rate-distortion limit of  $S/D = 2^{2R}$ . The difference in SNR (horizontal axis) is 6 to 7 dB. Note that coded modulation can achieve a coding gain of several dB, and would thus narrow this performance difference.

## VI. DISCUSSION

In a single-carrier system, it is possible to use coded modulation to improve the performance. Of course, it is also possible to use coded modulation on each individual



**Modulation Scheme:**  
**2 bits: 2 × BPSK**  
**3 bits: BPSK + 2 × QPSK**  
**4 bits: 4 × QPSK**  
**5 bits: 2 × QPSK + 3 × 8-QAM**  
**6 bits: QPSK + 3 × 8-QAM + 2 × 16-QAM**  
**7 bits: 3 × 8-QAM + 4 × 16-QAM**  
**8 bits: 8 × 16-QAM**

Fig. 6. Signal-to-overall distortion ratio  $S/D$ , as a function of the average SNR  $\rho_T$  of an AWGN channel. As the average SNR increases, the number of bits is increased to improve  $S/D$ , and modulation constellations having a greater number of points are required. Different bits can be transmitted over subchannels using different modulation schemes to improve the performance.

subchannel of a multicarrier system. If both single-carrier and multicarrier systems use the same type of coded modulation schemes, the effect is simply to shift the  $x$ -axes in Figs. 3–6 (except the distortion limit curve). In a single-carrier system, it is also possible to use multilevel coded modulation [35]–[36] or unequal error protection codes [37]–[38] to provide unequal error protection to different bits; however, this may be complicated to implement and lacks the flexibility of multicarrier modulation.

In the numerical examples in Section III to Section V, for simplicity, we limited our discussion to an AWGN channel with uniform noise density. However, the power-allocation algorithm in Section II-C is a general result that can be applied to all kind of channels, as long as the BER function, its derivative, and the inverse of its derivative can be found either analytically or numerically. However, we might expect the results to become more complicated for channels other than the simple AWGN channel.

The multicarrier modulation system in Fig. 2 is a special case of a more general class of multicarrier systems. The carriers need not be sinusoids, but can be any collection of mutually orthogonal functions. A generalized multicarrier system uses carriers  $\varphi_1, \dots, \varphi_N$ , where

$$\int_0^T \varphi_i(t) \varphi_j(t) dt = \delta_{ij} \quad (23)$$

where  $T$  is the symbol period. The multiplexed signal is

$$y(t) = \sum_{m=1}^N a_m \varphi_m(t) \quad 0 \leq t < T \quad (24)$$

where  $a_m$  is the modulation signal. For the system shown in Fig. 2,  $\varphi_m = e^{j2\pi f_m t} / \sqrt{T}$  and  $a_m$  is one of the values in the QAM constellation.

Any generalized multicarrier modulation can be used for our combined source-channel coding scheme. The power-allocation scheme will change the power of each carrier by changing the amplitude of  $a_m$ . For example, a time-division multiplexed system represents a simple example of a generalized multicarrier system in which

$$\varphi_m(t) = \begin{cases} \sqrt{N/T} & (m-1)T/N \leq t < mT/N \\ 0 & \text{otherwise.} \end{cases} \quad (25)$$

With time-division multiplexing, one could employ different constellation in each of the  $N$  time slots. However, we suggest that this may not be a desirable scheme, because the average powers transmitted within each time slot would not be the same. In addition, a synchronous code-division multiple-access (CDMA) system can also be considered as a “generalized” multicarrier system.

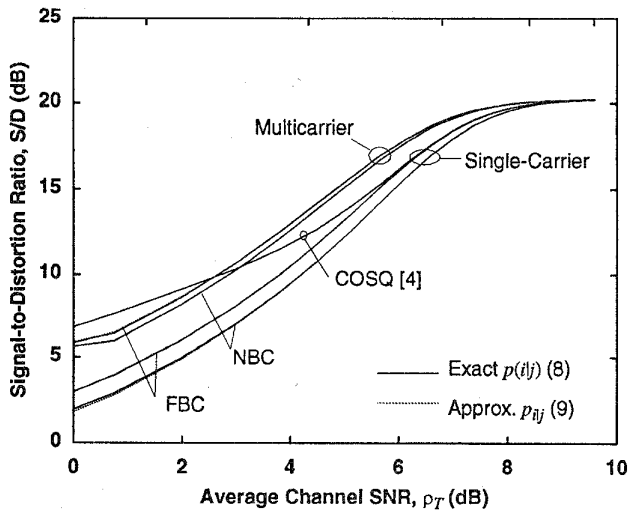


Fig. 7. Performance comparison of a 4 b scalar quantizer for a Gaussian source, where the quantized output is transmitted via single-carrier or multicarrier channels. For comparison, Lloyd–Max-quantized data are transmitted over single-carrier or multicarrier systems, and the COSQ [4] is also utilized.

It is worthwhile to compare our results with those of other combined source-channel coding approaches [3]–[8]. In general, in the results of [3]–[8], the improvement obtained using combined source-channel coding increases as the BER increases. However, with our approach, in the low-SNR region the improvement decreases as the BER increases (or the SNR decreases), which can be seen in Fig. 4. Therefore, in the very low-SNR region (e.g., SNR < 1 dB or BER > 0.1, depending on the number quantization levels and modulation scheme), the approaches in [3]–[8] may outperform our scheme. Fig. 7 shows a comparison between our multicarrier result and the channel-optimized scalar quantizer (COSQ) of [4] for 4 b quantizers. For the COSQ in [4], for BER's of 0.005 ( $\rho_T = 5.21$  dB) and 0.01 ( $\rho_T = 4.32$  dB), values of  $S/D$  are 14.15 dB and 12.30 dB, respectively. It can be seen in Fig. 7 that using FBC, our scheme achieves values of  $S/D$  that are 15.65 dB and 13.62 dB for single-carrier BER's of 0.005 and 0.01, respectively. For this range of SNR's, our scheme is more than 1 dB better than the scheme in [4]. At a single-carrier BER of 0.05, the scheme in [4] yields a  $S/D$  of 7.81 dB, while our scheme yields  $S/D$  of 7.49 dB; thus, our scheme is 0.3 dB worse than the scheme of [4]. Therefore, we conclude that the performance of our scheme is most competitive at "moderate" SNR's.

In obtaining the results of Figs. 3–6, we use the approximate transition probabilities (9) and assume that the exact transition probabilities (8) would also yield the same results. Fig. 7 shows the comparison between the results obtained using the approximate transition probabilities (9) and the exact transition probabilities (8). The difference is observable in the low-SNR range, but is insignificant in the range of SNR's considered in Fig. 7. However, for very small SNR's (for example, less than 5 dB), the difference may be significant. But we are not concerned with this very low-SNR range in this paper. Additional numerical results show that the difference becomes

larger when the number of quantized bits decreases (e.g., to 3 or 2 b).

## VII. CONCLUSION

We have proposed a combined source-channel coding scheme using multicarrier modulation. By changing the power and modulation of subchannels carrying different bits of the quantized signal, the channel-induced distortion can be minimized. An algorithm for the allocation of subchannel power has been derived. The asymptotic gain of signal-to-channel-induced-distortion ratio has been derived for an AWGN channel.

Optimal scalar quantizers using natural binary and folded binary codes have been considered. The use of identical modulation constellation for all subchannels was considered first, and the use of different constellations for different subchannels was also discussed. In a numerical example of a Gaussian source, using multicarrier modulation, we obtain a performance improvement of multicarrier over single-carrier modulation as large as 13 dB for an 8 b scalar quantizer. Quantizers using a smaller number of bits yield a smaller improvement.

Both full-search and binary tree search vector quantizer have been designed, and a natural binary coding scheme has been employed. For a vector quantizer using 2 b/sample, the improvement in overall signal-to-distortion ratio lies in the range between 0.3 and 0.8 dB, depending on the dimension of the vector quantizer and whether full-search or tree-search quantizer is employed.

Finally, it should be noted that we have made exclusive use of optimal quantizers to minimize the distortion between codewords and the original signal, and then, holding the choice of quantizer fixed, have changed the modulation scheme (channel encoding) to maximize signal-to-distortion ratio. This has simplified the analysis, but it raises the question of whether improved quantizer design might provide a significant further reduction of the distortion between the reconstructed signal and the original signal. While we have not attempted to design quantizers jointly with the modulation scheme, we suspect that this will lead to only a small additional improvement, especially for the range of SNR that is of practical interest.

## REFERENCES

- [1] C. E. Shannon, "A mathematical theory of communication," *Bell Syst. Tech. J.*, vol. 27, pp. 379–423, pp. 623–656, 1949.
- [2] ———, "Coding theorems for a discrete source with a fidelity criterion," in *IRE Nat. Conv. Rec.*, Mar. 1959, pp. 142–163.
- [3] A. Kurtenbach and P. Wintz, "Quantizing for noisy channels," *IEEE Trans. Commun. Technol.*, vol. 17, pp. 291–302, 1969.
- [4] N. Farvadin and V. Vaishampayan, "Optimal quantizer design for noisy channels: An approach to combined source-channel coding," *IEEE Trans. Inform. Theory*, vol. 22, pp. 461–470, 1986.
- [5] E. Ayanoglu and R. M. Gray, "The design of joint source and channel trellis waveform coders," *IEEE Trans. Inform. Theory*, vol. IT-33, pp. 855–865, 1987.
- [6] N. Farvadin and V. Vaishampayan, "On the performance and complexity of channel-optimized vector quantizers," *IEEE Trans. Inform. Theory*, vol. 37, pp. 155–160, 1991.
- [7] N. Phambo, N. Farvadin, and T. Moriya, "A unified approach to tree-structured and multistage vector quantization for noisy channels," *IEEE Trans. Inform. Theory*, vol. 39, pp. 835–850, 1993.

- [8] M. Wang and T. R. Fischer, "Trills-coded quantization designed for noisy channels," *IEEE Trans. Inform. Theory*, vol. 40, pp. 1803-1817, 1994.
- [9] S. B. Weinstein and P. M. Ebert, "Data transmission by frequency-division multiplexing using the discrete fourier transform," *IEEE Trans. Commun. Technol.*, vol. COM-19, pp. 628-634, 1971.
- [10] L. J. Cimini Jr., "Analysis and simulation of a digital mobile channel using orthogonal frequency division multiplexing," *IEEE Trans. Commun.*, vol. COM-33, pp. 665-675, 1985.
- [11] I. Kalet, "The multitone channel," *IEEE Trans. Commun.*, vol. 37, pp. 119-124, 1989.
- [12] W. Y. Chen and D. L. Waring, "Applicability of ADSL to support video dial tone in the copper loop," *IEEE Commun. Mag.*, vol. 32, pp. 102-109, May 1994.
- [13] J. A. C. Bingham, "Multicarrier modulation for data transmission: An idea whose time has come," *IEEE Commun. Mag.*, pp. 5-14, May 1990.
- [14] J. S. Chow, J. C. Tu, and J. M. Cioffi, "A discrete multitone transceiver system for HDSL applications," *IEEE J. Select. Areas Commun.*, vol. 9, pp. 895-908, 1991.
- [15] K. D. Kammeyer, U. Tuisel, H. Schulze, and H. Bockmann, "Digital multicarrier-transmission of audio signals over mobile radio channels," *European Trans. Telecommun. Related Technol.*, vol. 3, pp. 243-253, 1992.
- [16] P. J. Tourtier, R. Monnier, and P. Lopez, "Multicarrier modem for digital HDTV terrestrial broadcasting," *Signal Processing: Image Commun.*, vol. 5, pp. 379-403, 1993.
- [17] Y. Wu and B. Carson, "Digital television terrestrial broadcasting," *IEEE Commun. Mag.*, vol. 32, pp. 46-52, May 1994.
- [18] C. Petrovic, W. Roehr, and D. W. Cameron, "Multicarrier modulation for narrowband PCS," *IEEE Trans. Veh. Technol.*, vol. 43, pp. 856-862, 1994.
- [19] H. Sari, G. Karam, and I. Jeanchaude, "Transmission techniques for digital terrestrial TV broadcasting," *IEEE Commun. Mag.*, pp. 100-109, Feb. 1995.
- [20] S. P. Lloyd, "Least squares quantization in PCM," Bell Laboratories Technical Note, 1957, *IEEE Trans. Inform. Theory*, vol. IT-28, pp. 129-137, 1982.
- [21] J. Max, "Quantizing for minimum distortion," *IRE Trans. Inform. Theory*, vol. IT-6, pp. 7-12, Mar. 1960.
- [22] R. M. Gray, "Vector quantization," *IEEE Acoust. Speech Signal Processing Mag.*, vol. 1, pp. 4-29, Apr. 1984.
- [23] A. Gersho and R. M. Gray, *Vector Quantization and Signal Compression*. Boston, MA: Kluwer, 1992.
- [24] R. E. Totty and G. C. Clark, "Reconstruction error in waveform transmission," *IEEE Trans. Inform. Theory*, vol. IT-13, pp. 336-338, 1967.
- [25] N. Farvardin, "A study of vector quantization for noisy channels," *IEEE Trans. Inform. Theory*, vol. 36, pp. 799-809, 1990.
- [26] N. Rydbeck and C.-E. Sundberg, "Analysis of digital errors in nonlinear PCM systems," *IEEE Trans. Commun.*, vol. COM-24, pp. 59-65, 1976.
- [27] C.-E. Sundberg, "The effect of single-bit errors in standard nonlinear PCM systems," *IEEE Trans. Commun.*, vol. COM-24, pp. 1062-1064, 1976.
- [28] R. Steele, C.-E. Sundberg, and W. C. Wong, "Transmission errors in companded PCM over Gaussian and Rayleigh fading channels," *AT&T Bell Lab. Tech. J.*, vol. 63, pp. 955-990, 1984.
- [29] J. G. Proakis, *Digital Communications*, 3rd ed. New York: McGraw-Hill, 1995.
- [30] P. F. Panter and W. Dite, "Quantization distortion in pulse-count modulation with nonuniform spacing of levels," in *Proc. IRE*, Jan. 1951, vol. 39, pp. 44-48.
- [31] B. Smith, "Instantaneous companding of quantized signals," *Bell Syst. Tech. J.*, vol. 36, pp. 653-709, 1957.
- [32] E. Bedrosian, "Weighted PCM," *IRE Trans. Inform. Theory*, vol. IT-4, pp. 45-49, 1958.
- [33] L. Linde, A. Buzo, and R. M. Gray, "An algorithm for vector quantizer design," *IEEE Trans. Commun.*, vol. COM-28, pp. 84-95, 1980.
- [34] J. Markhoul, S. Roucos, and H. Gish, "Vector quantization in speech coding," *Proc. IEEE*, vol. 73, pp. 1551-1558, 1985.
- [35] L.-F. Wei, "Coded modulation with unequal error protection," *IEEE Trans. Commun.*, vol. 41, pp. 1439-1449, 1993.
- [36] A. R. Calderbank and N. Seshadri, "Multilevel codes for unequal error protection," *IEEE Trans. Inform. Theory*, vol. 39, pp. 1234-1248, 1993.
- [37] B. Masnick and J. Wolf, "On linear unequal error protection codes," *IEEE Trans. Inform. Theory*, vol. IT-13, pp. 600-607, 1967.
- [38] J. Hagenauer, "Rate-compatible punctured convolutional codes (RCPC codes) and their applications," *IEEE Trans. Commun.*, vol. 36, pp. 389-400, 1988.



**Keang-Po Ho** (S'92-M'95) received the B.S. degree from National Taiwan University in 1991 and M.S. and Ph.D. degrees from the University of California at Berkeley in 1993 and 1995, respectively, all in electrical engineering.

From 1992 to 1995, he was a Research Assistant in the Department of Electrical Engineering and Computer Sciences of the University of California at Berkeley, conducted research in communication systems, optical communication, communication theory, digital signal processing, image and video transmission. During the summer of 1994, he worked in IBM T.J. Watson Research Center, Hawthorne, NY on all-optical networks. He has been in Bellcore, Red Bank, NJ since 1995 as a Research Scientist. His interests include optical communication systems, video transmission systems, broadband access, and communication theory.



**Joseph M. Kahn** (M'87) received the A.B., M.A., and Ph.D. degrees in physics from the University of California at Berkeley in 1981, 1983, and 1986, respectively. His Ph.D. thesis was entitled "Hydrogen-Related Acceptor Complexes in Germanium."

He is Professor in the Department of Electrical Engineering and Computer Sciences at the University of California at Berkeley. From 1987-1990, he was a Member of Technical Staff in the Lightwave Communications Research Department of AT&T Bell Laboratories at Crawford Hill Laboratory in Holmdel, NJ, where he performed research on multi-gigabit-per-second coherent optical fiber transmission systems and related device and subsystem technologies. He demonstrated the first BPSK-homodyne optical fiber transmission system, and achieved world records for receiver sensitivity in multi-gigabit-per-second systems. He joined the faculty of the University of California at Berkeley in 1990, where his research interests include infrared and radio wireless communications, and optical fiber communications. He is serving currently as a Technical Editor of *IEEE PERSONAL COMMUNICATIONS MAGAZINE*.

Dr. Kahn is a recipient of the National Science Foundation Presidential Young Investigator Award.